Reflection of electromagnetic radiation from structured metallic magnets

R. E. Camley,* T. J. Parker, and S. R. P. Smith

Department of Physics, University of Essex, Colchester C04 3SQ, United Kingdom

(Received 10 October 1995)

We present theoretical calculations for the reflection of electromagnetic waves from structured magnetic materials which are metallic. Normally one expects that electromagnetic probes of metallic materials are not helpful because of the high background reflectivity. We show that if the electron motion can be limited by the structuring then one can see distinct features in the reflectivity which arise from the magnetic excitations. This is in sharp contrast to the case for unstructured metallic magnetic materials where the reflectivity is near unity. The calculations are carried out primarily within effective-medium theory, but by an exact calculation in a special case, we show that the general results hold true for parameters well beyond the limits of validity of effective-medium theory.

I. INTRODUCTION

One of the most common methods used to characterize the magnetic, electronic, and elastic properties of materials is to measure the reflectivity of electromagnetic radiation from the material. For example, we note recent reflectivity studies of semiconductor superlattices have given information on surface charge densities.[1] Similarly reflection of infrared radiation has given information on the temperature dependence of the linewidth in insulating antiferromagnets.[2-4]

Unfortunately this method can not be used with many magnetic materials because they are also metallic. As a result, the electron motion induced by the incident wave near the surface of the sample screens the interior of the sample from interacting with the wave. In this case the reflectivity remains near unity, independent of the existence of any magnetic excitation. This result also depends on the linewidth for the magnetic excitation. In principle if the linewidth were narrow enough (<20 G) magnetic features could be seen. However, most magnetic, metallic materials seem to have quite large linewidths. We note that the method discussed here shows significant magnetic features even in the presence of very large linewidths.

Thus to study the magnetic excitations in metallic systems one needs to reduce the screening effects of the electron motion. One way to do this is to prevent large scale eddy currents by fabricating a striped or grooved structure as shown in Fig. 1. If the stripes are perpendicular to the electric field, then the electron motion is limited and the screening is significantly reduced.

In this paper we calculate the electromagnetic reflectivity from grooved metallic magnetic films. We consider particular geometries so that the screening effect of the electron motion is largely prevented, while the interaction of the electromagnetic wave with the magnetic excitations in the material is still strong. We present calculations for both metallic ferromagnets applicable to materials such as Fe, Co, or Gd for example, and for metallic antiferromagnets, Cr for example. In both cases we will see that without the grooves the electromagnetic reflectivity is very close to 1. However, when the grooves are present, the reflectivity is significantly reduced and a distinct magnetic signature, tunable with ap-

plied magnetic field, is found in the reflectivity.

Our calculations are done within the effective-medium approximation,[5] a method which has had much application in semiconductor[6,7] and magnetic[8-12] layered structures. In this approximation the grooved material is replaced by an effective medium which has a dielectric tensor and permeability tensor which depend on the fraction of the material which is magnetic and conducting. The resulting reflectivity calculations are straightforward and relatively simple. However, the effective-medium approximation makes use of certain assumptions — essentially that the amplitudes of the E and B fields do not vary significantly across an individual material. It is of interest to see if the basic results persist in the range of parameters where effective medium theory does not hold. We have therefore carried out a calculation where the grooved material is treated as a true superlattice, and the electromagnetic modes within this superlattice are calculated exactly. This calculation gives an effective dielectric tensor which depends not only on the fraction of the material which is conducting but also on the exact size of the conducting and nonconducting materials. The resulting reflectivity shows
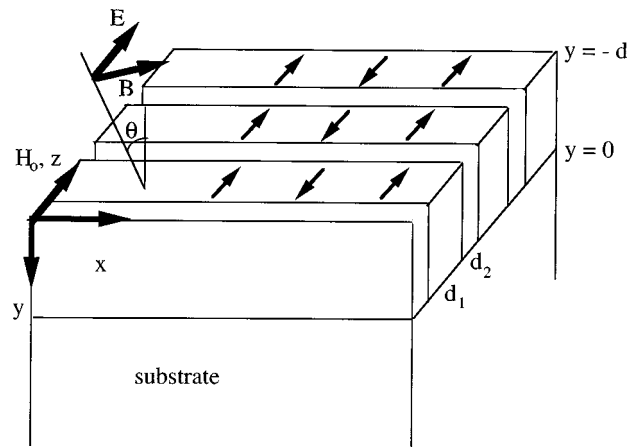

FIG. 1. Geometry considered in this paper. The E field of the wave is along the z axis as is the static external magnetic field H_0. d_1 is the width of the magnetic stripe and d_2 is the width of the groove. The film has a thickness d.

that the magnetic excitations can still be seen for structures where the effective-medium approximation does not hold. The magnetic contribution to the reflectivity is, however, somewhat reduced, when compared to the effective-medium calculation.

The methods discussed in this paper should be applicable to a wide range of materials and for a wide range of frequencies. We will generally refer to frequencies in terms of wave numbers, $\omega/2\pi c$. The excitation frequencies for antiferromagnets often lie in the infrared, around 37 cm^{-1} for Cr. Rare earth magnetic systems[12] are also expected to have excitations in the 10–40 cm^{-1} range. Magnetic excitations for ferromagnets lie typically in the 10–30 GHz range (1 GHz ≈ 0.3 cm^{-1}), however, exchange influenced spin wave modes may have much higher frequencies.

The paper is outlined as follows. In Sec. II the theoretical results for reflectivity are obtained within the effective-medium approximation. In Sec. III we present results for reflection from grooved antiferromagnets and ferromagnets. In Sec. IV we develop a method for going beyond effective medium and apply the results to reflection from antiferromagnets as an example. In Sec. V we present conclusions.

II. THEORY

The geometry is illustrated in Fig. 1. The electric field is in the z direction, always parallel to the surface and perpendicular to the spacer films/grooves. The applied static external magnetic field, H_0, is also in the z direction. The effective medium film has thickness d and sits on a thick nonmagnetic substrate. The width of the metallic strips is d_1 and the width of the nonmetallic strips is given by d_2.

The dielectric tensor for the metal is taken to be diagonal and have value ϵ_1. Similarly the dielectric tensor for the nonmetallic region is also diagonal and has a value ϵ_2. Finally the dielectric constant for the substrate is denoted by ϵ_s. When we consider the alternating metallic/nonmetallic region as a layered structure, we may obtain a dielectric tensor for a resulting effective material given by[5,6]

$$\epsilon = \begin{pmatrix} \epsilon_{xx} & & \\ & \epsilon_{yy} & \\ & & \epsilon_{zz} \end{pmatrix}$$

$$= \begin{pmatrix} f_1\epsilon_1+f_2\epsilon_2 & 0 & 0 \\ 0 & f_1\epsilon_1+f_2\epsilon_2 & 0 \\ 0 & 0 & \left(\dfrac{f_1}{\epsilon_1}+\dfrac{f_2}{\epsilon_2}\right)^{-1} \end{pmatrix}, \quad (1)$$

where f_1 is the fraction of the film occupied by the metallic magnet and is given by

$$f_1 = \frac{d_1}{d_1+d_2}. \quad (2)$$

Similarly f_2 is the fraction of the film which is grooved and is given by

$$f_2 = \frac{d_2}{d_1+d_2}. \quad (3)$$

A key feature of the effective-medium dielectric tensor is the form for ϵ_{zz}. Since ϵ_1 for metal is large (and imaginary), ϵ_{zz} is approximately ϵ_2/f_2 and nearly independent of the metallic material. As we will see, it is this component of the dielectric tensor that is relevant in the reflection calculation, and as a result the problems with the metallic reflectivity are eliminated.

The magnetic permeability tensor for the magnet has the form

$$\mu = \begin{pmatrix} \mu_{xx} & \mu_{xy} & 0 \\ \mu_{yx} & \mu_{yy} & 0 \\ 0 & 0 & 1 \end{pmatrix}, \quad (4)$$

while in the grooves and the substrate the permeability is unity. The precise expressions for the components of the permeability tensor depend on the material, however, the general structure for the tensor is the same for both ferromagnets and uniaxial antiferromagnets when the applied field is in the z direction. The permeability tensor for the effective medium formed by the grooves and the magnetic materials is then given by[10,11]

$$\mu = \begin{pmatrix} \mu_1 & i\mu_2 & 0 \\ -i\mu_2 & \mu_1 & 0 \\ 0 & 0 & 1 \end{pmatrix}$$

$$= \begin{pmatrix} f_1\mu_{xx}+f_2 & f_1\mu_{xy} & 0 \\ f_1\mu_{yx} & f_1\mu_{yy}+f_2 & 0 \\ 0 & 0 & 1 \end{pmatrix}. \quad (5)$$

The calculation for the reflectivity is straightforward. We assume electric fields in the three regions are given by

$$\vec{E}(\vec{x},t)=\hat{z}(1\,e^{ik_\perp(y+d)}+\mathrm{Re}^{-ik_\perp(y+d)})e^{i(kx-\omega t)} \quad (6)$$

above the film,

$$\vec{E}(\vec{x},t)=\hat{z}(E_+e^{iqy}+E_-e^{-iqy})e^{i(kx-\omega t)} \quad (7)$$

in the film,

$$\vec{E}(\vec{x},t)=\hat{z}\mathrm{Te}^{iQy}e^{i(kx-\omega t)} \quad (8)$$

in the substrate.

The parallel component of the wave vector, k, is the same in all three regions. The perpendicular components are found by using the dispersion relation for each medium separately. One finds

$$k_\perp = \sqrt{\omega^2/c^2-k^2}, \quad (9)$$

$$q = \sqrt{[(\mu_1^2-\mu_2^2)/\mu_1](\epsilon_{zz}\omega^2/c^2)-k^2}, \quad (10)$$

$$Q = \sqrt{(\omega^2/c^2)\epsilon_s-k^2}. \quad (11)$$

We note that for the effective medium film only the ϵ_{zz} appears. This is important because ϵ_{zz} is not dominated by the metallic conductivity as discussed earlier.

For each electric field one may find an associated H field through the use of Maxwell's equations. Using $\nabla \times \vec{E} = -(1/c)\partial \vec{B}/\partial t$ and $\vec{B} = \vec{\mu}\vec{H}$ we obtain a general connection between E and H_x to be

$$H_x(x,t) = \frac{c}{i\omega(\mu_1^2 - \mu_2^2)}\left[\mu_1 \frac{\partial E}{\partial y} + i\mu_2 \frac{\partial E}{\partial x}\right]. \quad (12)$$

This equation must be applied with the appropriate permeabilities in each region.

One now applies the boundary conditions. Continuity of H_x at $y=0$ and $y=-d$ leads to

$$QT = k_+ E_+ + k_- E_-, \quad (13)$$

$$k_\perp(1-R) = k_+ e^{-iqd}E_+ + k_- e^{+iqd}E_-, \quad (14)$$

where

$$k_\pm = \frac{\pm\mu_1 q + i\mu_2 k}{\mu_1^2 - \mu_2^2}. \quad (15)$$

Similarly, continuity of tangential E at the boundaries gives

$$E_+ + E_- = T, \quad (16)$$

$$1 + R = E_+ e^{-iqd} + E_- e^{+iqd}. \quad (17)$$

After some algebra, the four boundary condition equations yield the amplitude R

$$R = \frac{C-1}{C+1}, \quad (18)$$

where

$$C = k_\perp\left[\frac{Fe^{-2iqd}+1}{k_+ Fe^{-2iqd}+k_-}\right] \quad (19)$$

and

$$F = -\left(\frac{Q-k_-}{Q-k_+}\right). \quad (20)$$

Equation (18) gives the amplitude R for the reflected wave when the incident wave has an amplitude of unity. We thus take R^*R as our measure of the reflectivity.

III. RESULTS

We first present results for a model uniaxial antiferromagnet which as a resonance frequency similar to Cr. The elements of the permeability tensor for an antiferromagnet are given by[13]

$$\mu_{xx} = \mu_{yy} = 1 - 4\pi M H_a(X+Y), \quad (21)$$

$$\mu_{xy} = -\mu_{yx} = 4\pi M H_a(Y-X), \quad (22)$$

where

$$X = [(\omega + \gamma H_0 + i\gamma\Delta H)^2 - \omega_0^2]^{-1}, \quad (23)$$

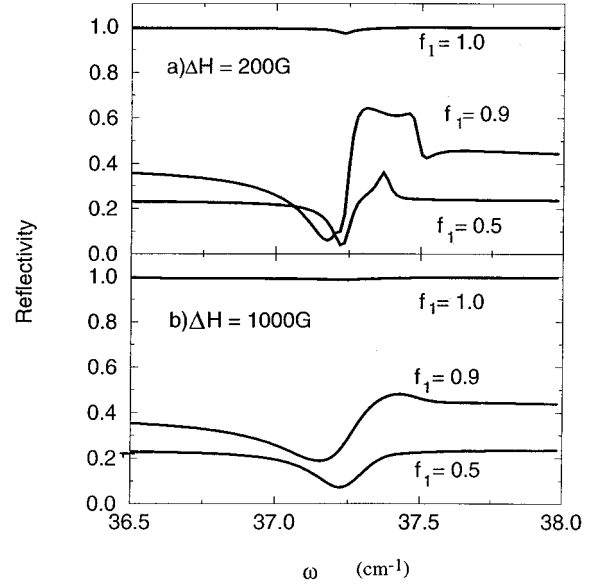$$Y = [(\omega - \gamma H_0 + i\gamma\Delta H)^2 - \omega_0^2]^{-1}. \quad (24)$$

FIG. 2. Reflectivity from a structured antiferromagnet as a function of frequency for different values of f_1. The parameters for the calculation are $d=10$ μm and $H_0=0$. $f_1=1$ corresponds to the case of a uniform metallic and magnetic film.

Here ω_0 is the antiferromagnetic resonance frequency given by

$$\omega_0 = \gamma\sqrt{H_a(H_a + 2H_e)}, \quad (25)$$

which is appropriate for an uniaxial antiferromagnet. In the above H_e is the exchange field, H_a is the anisotropy field, M is the saturation magnetization of an individual sublattice, γ is the gyromagnetic ratio, and ΔH is the resonance linewidth.

For our metallic antiferromagnet we take $H_e = 434$ kG, $H_a = 149$ kG, and $M = 0.6$ kG. The dielectric function for the metal is given by

$$\epsilon_1 = 1 + i\frac{\sigma}{\omega\epsilon_0}, \quad (26)$$

where the right-hand side is all given in terms of mks units for convenience. Note that the $+$ sign in the previous equation depends on our choice of sign for the wave where we have taken $\exp(-i\omega t)$. The conductivity is taken to be 0.78×10^7 $(\Omega m)^{-1}$. In our examples we will also take $\epsilon_2 = 1$, and $\epsilon_s = 5$. We have taken the thickness of the effective medium film to be 10 μm, although thicknesses down to 1 μm give reasonable signals. The strength of the signal can also be tuned somewhat by altering the dielectric constant of the substrate. We have also taken the angle of incidence to be 45° in all cases.

In Fig. 2 we present results for the reflectivity as a function of frequency depending on the fraction of the material occupied by the magnet and on the linewidth of the magnetic excitation. Generally we expect that values around $f_1 = 0.9$ will be the best choice to see the magnetic excitation. This interrupts the motion of the electrons and thus reduces the screening, but the magnetic response is basically unchanged. In Fig. 2(a), the $f_1 = 0.9$ curve shows the general features associated with a magnetic excitation in an antiferromagnet.
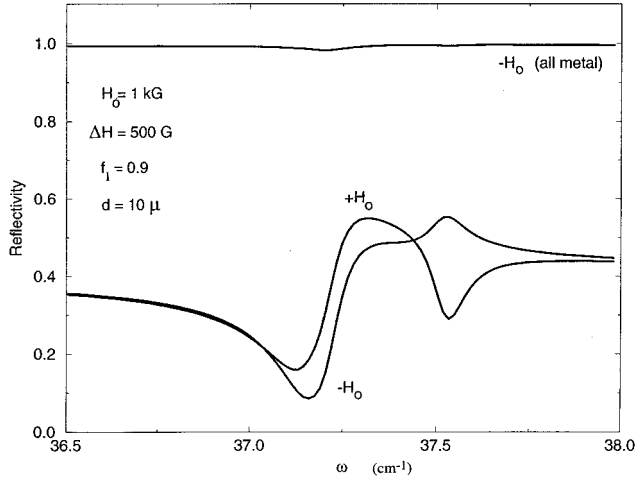
FIG. 3. Reflectivity from a structured antiferromagnet as a function of frequency for $+H_0$ and $-H_0$. The additional parameters for the calculation are $d=10$ μm, $f_1=0.9, \Delta H=500$ G, and $H_0=1$ kG.

The dip at low frequencies corresponds to the magnetic Brewster angle; the nearly flat peak corresponds to a reststrahl band — a gap between bulk magnetic polariton bands. The slight decrease in reflectivity through this band comes from the change in penetration depth with frequency. At frequencies just past the resonance, μ_1 is negative and decreasing in magnitude. This decrease leads to a greater penetration depth and so the reflectivity is reduced. For the low damping case seen in Fig. 2(a), it is clear that the $f_1=0.5$ case has a different shape than the $f_1=0.9$ case. This is because f_1 is now small enough that the magnetic permeability is also influenced by the grooves. This generally reduces the width of the reflectivity peak. It is interesting to note that changing the f_1 parameter also sets the ''background'' reflectivity.

Figure 2(b) shows equivalent results for a higher linewidth of $\Delta H=1000$ G. In this case the signal from the completely metallic structure is essentially constant. It is obvious that there is a significant advantage for the effective medium material which continues to show clear signals even at this high linewidth. It is not obvious what a typical linewidth for an antiferromagnetic metal might be, but linewidths in ferromagnetic thin films[14] can be as low as 50 G but are typically in the 200–300 G range.

In Fig. 3 we show the reflectivity as a function of frequency in an applied magnetic field. In the presence of a magnetic field the reflectivity can be distinctly nonreciprocal in that reversing the direction of propagation changes the reflectivity.[4] In our geometry reversing propagation is equivalent to a reversal of the applied field. We see that the nonreciprocity is very clearly displayed in the results shown in Fig. 3 for the effective medium material. However, the equivalent metallic film displays virtually no structure in the reflectivity.

We now turn to a study of a model ferromagnet. In this case the permeability tensor elements are given by[15]

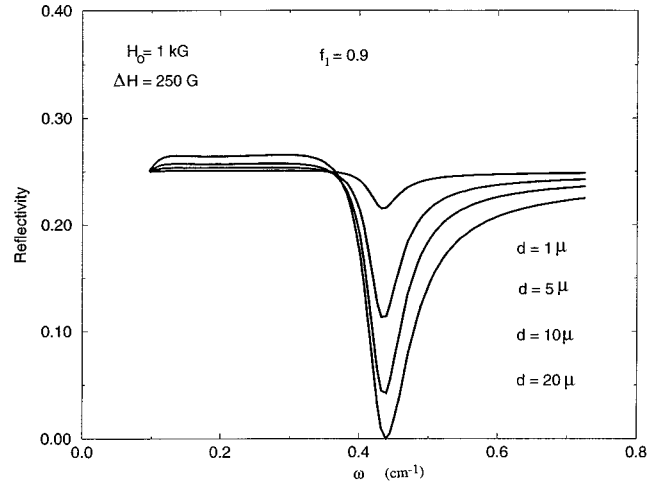$$\mu_{xx}=1-\frac{4\pi H_0 M}{(\omega/\gamma+i\Delta H)^2-H_0^2}, \tag{27}$$

FIG. 4. Reflectivity from a structured ferromagnet as a function frequency for different thicknesses, d, of the effective-medium film.

$$\mu_{xy}=-\mu_{xy}=i\frac{4\pi\omega M}{(\omega/\gamma+i\Delta H)^2-H_0^2}. \tag{28}$$

We use the following parameters: $M=1.7$ kG and $\sigma=1\times10^7$ $(\Omega$ m$)^{-1}$. For frequencies in the 10–20 GHz range this gives a skin depth due to the metallic conductivity which is on the order of 1 μm

In Fig. 4 we examine the reflectivity as a function of the thickness, d, of the effective medium film. For the structured material, the reflectivity shows a significant change even for films as thin as 1 μm. In contrast, a completely metallic film shows, again, a reflectivity which is independent of frequency and thus has no information about magnetic excitation. For the structured ferromagnet, the dip in the reflectivity occurs very close to the frequency which defines the upper edge of the bulk spin wave band, $\omega_B=\gamma(H_0(H_0+4\pi M))^{1/2}$. Because of the large value of M this frequency can be quite high compared to that for garnets [M for YIG (yttrium iron garnet) is around 130 G], and thus the structured ferromagnet could be promising for high frequency signal processing.

We note that the thickness required to see a reasonable reflectivity depends critically on the magnetization. This is because the components of the permeability tensor in the ferromagnet are essentially proportional to M. As a result ferromagnets with smaller values of M, for instance Ni where $M=480$ G, would need significantly thicker films to produce the same size reflectivity signal.

We have examined how the reflectivity signal depends on the important parameters of the physical system. In Fig. 5 we study how the reflectivity depends on the linewidth. We see a very sharp signal at a linewidth of 100 G. As the linewidth is increased, the dip becomes broader, but even at a linewidth of 500 G there is still a significant signal. The frequency of the reflectivity dip can be shifted by the external field as we have seen above. Our calculations show that as the field is increased from 1 kG to 10 kG (with $d=5\mu$m, $f_1=0.9$, and $\Delta H=250$ G) the dip becomes only slightly deeper.

One finds nonreciprocal reflection in the ferromagnet as well as in the antiferromagnet. In Fig. 6 we show how the reflectivity changes when the propagation direction is re-
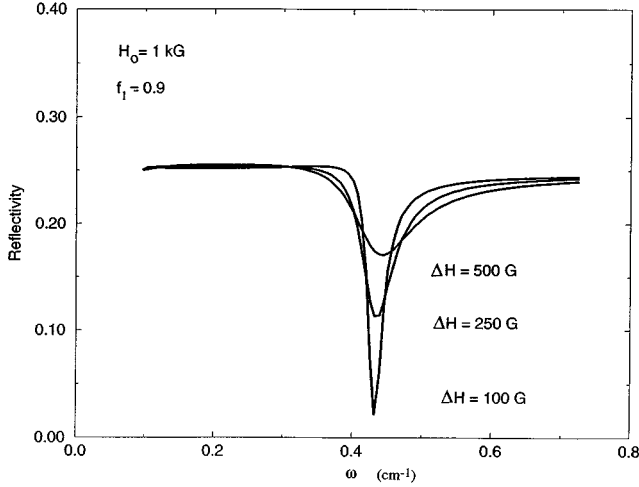
FIG. 5. Reflectivity from a structured ferromagnet as a function of frequency for different linewidths. A distinct magnetic signal is seen even for fairly large linewidths.

versed. Note that the dip in reflectivity is slightly shifted depending on the propagation direction. For the parameters used here, the major factor controlling the nonreciprocity is the thickness of the effective medium film. A thicker film leads to a much larger nonreciprocity.

In an effort to keep the problem simple and concentrate on the main ideas, we have not included a number of factors in our calculations for the ferromagnet. For example the influence of bulk and surface anisotropy fields has been neglected.[16,17] In addition, we have not included the effects of static demagnetizing fields. Anisotropy fields and demagnetizing fields could be substantial and produce shifts in the resonance frequency. Nonetheless, the general features demonstrated in our calculation are expected to remain. The calculation of the demagnetizing fields depends critically on the exact geometry, the width of the cut and the overall dimension of the sample, and are beyond the scope of the present work. Demagnetizing fields are not expected to play as large a role in the antiferromagnet when the surfaces contain both up and down spins.
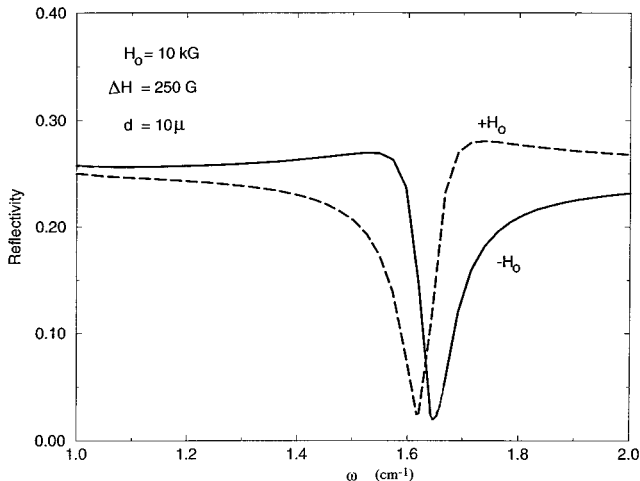

FIG. 6. Reflectivity from a structured ferromagnet as a function of frequency for $+H_0$ and $-H_0$.

IV. BEYOND EFFECTIVE-MEDIUM THEORY

As discussed in the Introduction, the use of effective-medium theory implies that the electromagnetic fields within a given material do not change too rapidly. In this section we explore how well the idea of using grooves to reduce the conductivity works when effective-medium theory is not valid.

We consider a simple geometry in which a transverse-magnetic electromagnetic wave propagates parallel to the superlattice structure. Furthermore, we also restrict the calculation to a system where the permeability tensor in the magnetic material is diagonal. (An antiferromagnet in zero field satisfies this restriction.) With this geometry we can restrict the electromagnetic field components to H_y, E_z, and E_x. In this case the exact dispersion relation for propagation within the superlattice is given by[18]

$$1 = \cos(qd_1)\cos(k_\perp d_2) - \frac{(1+r^2)}{2r}\sin(qd_1)\sin(k_\perp d_2).$$

$$(29)$$

Here q and $k_\perp$ are given as previously in Eqs. (9) and (10) but with $\mu_2 = 0$ and μ_1 being that for the magnetic material only. The ratio, r, is given by

$$r = \frac{\epsilon_1 k_\perp}{\epsilon_2 q}.$$

$$(30)$$

Since q and $k_\perp$ are functions of k, Eq. (29) yields an implicit dispersion relation for ω as a function of k. In the effective-medium approximation one expands the sine and cosine terms in Eq. (29) based on the assumption that the arguments are small. One then obtains an explicit dispersion relation. In the simplest case this relation is then compared to that expected for an electromagnetic wave in a simple medium, i.e.,

$$\omega^2 = \frac{c^2 k^2}{\epsilon_{\text{eff}} \mu_{\text{eff}}}.$$

$$(31)$$

When the arguments of the sine and cosine terms in Eq. (29) are not small, the equation must be solved numerically. The resulting solution can then be compared to Eq. (31) and the product $\epsilon_{\text{eff}} \mu_{\text{eff}}$ can then be obtained. In our reflection calculation we see that not only is the product $\epsilon_{\text{eff}} \mu_{\text{eff}}$ required, but the individual values for ϵ_{eff} and μ_{eff} as well. To find this we initially solve Eq. (29) with the magnetism "turned off." This gives ϵ_{eff} for the structure. We then solve Eq. (29) again, but with the magnetism "turned on." This gives the product $\epsilon_{\text{eff}} \mu_{\text{eff}}$ and dividing this result by ϵ_{eff} then results in μ_{eff}.

In Fig. 7(a), we present results for μ_{eff} as a function of frequency for different values of d_1. In all the calculations $d_1 = d_2$ so the effective-medium filling factor $f_1 = 0.5$. At low d_1 values ($d_1 < 500$ Å) the effective-medium results and the exact results agree as expected. As d_1 is increased the magnetic resonance seen in μ_{eff} becomes weaker but is still present even for values of $d_1 = 5000$ Å. Physically the reason for this is that the electromagnetic wave does not penetrate
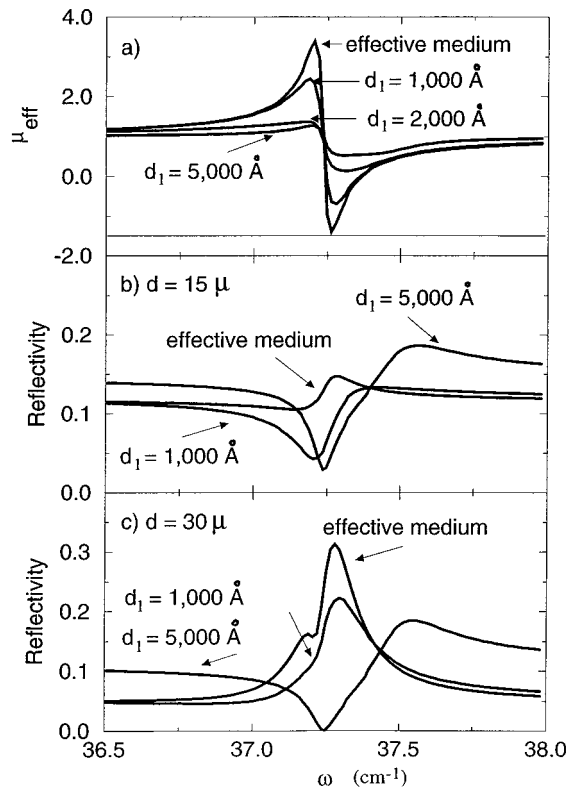
FIG. 7. Comparison of results from effective-medium theory and exact superlattice calculation. $\Delta H = 300$ G, $H_0 = 0$, and $f_1 = 0.5$ always so $d_1 = d_2$. (a) μ_{eff} as a function of frequency for different values of d_1 and d_2. As d_1 and d_2 get larger than the skin depth, μ_{eff} deviates from the effective-medium result, but a distinct magnetic signal remains. (b) Normal incidence reflectivity as a function of frequency for the effective-medium material and for $d = 15\mu$m. Here the $d_1 = d_2 = 0.5$ μm case actually gives a larger magnetic signal than the effective-medium result. (c) Normal incidence reflectivity as a function of frequency. Here $d = 30$ μm. For this thickness the effective-medium signal is larger than the $d_1 = d_2 = 0.5$ μm case.

completely into the magnetic material as the thickness d_1 gets larger than the skin depth. As a result the electromagnetic wave which propagates in the superlattice structure is less strongly influenced by the magnetic permeability and the resulting μ_{eff} is weaker.

In Figs. 7(b) and 7(c), we plot the normal incidence reflectivity for each of the different d_1 values considered in Fig. 7(a). Figure 7(b) corresponds to a $d = 15$ μm while Fig. 7(c) has $d = 30$ μm. Again for values of $d_1 < 500$ Å the reflectivity agrees with the effective-medium reflectivity. In Fig. 7(b), we see that the reflectivity calculated without the effective-medium approximation is actually larger than that found in the effective-medium method. More typically, however, the effective-medium calculation overestimates the reflectivity signal from the structure as is seen in Fig. 7(c). For

d_1 values above 1000 Å, the size of the magnetic reflectivity is reduced but is still clearly visible at $d_1 = 5000$ Å.

The skin depth for the metal is controlled, to a large extent, by the conductivity of the metal. For our model antiferromagnet, the skin depth (away from the magnetic resonance) is on the order of 1000 Å. Yet there is a clear magnetic signal in the reflectivity for structures which have widths on the order of 5000 Å.

V. SUMMARY AND CONCLUSIONS

We have seen in this paper that magnetic excitations can be seen in reflectivity measurements for metallic magnetic films. This is accomplished by interrupting the electron motion by introducing grooves into a magnetic film. If the grooves are narrow, then we can find reflection geometries where the measured magnetic permeability of the film will be essentially unchanged while the dielectric function is reduced significantly in magnitude.

The grooved structure discussed here could be made in several different ways. One could imagine growing a superlattice structure with alternating films of metal and insulator. This structure could be cut and looked at edge on. In this way one could get very narrow insulating films between thicker magnetic films. Alternatively, one could grow a uniform magnetic film and then cut grooves in the film by the usual photolithographic and etching methods. We have shown in our calculations for Cr that such a structure should work even if the widths of the grooves and the magnetic films are on the order of 0.5 μm, a width which should be obtainable by conventional means. If we are looking at excitations in rare-earth metals, the conductivity is significantly lower and we can expect that the corresponding structures could be even larger.

Finally, many other geometries remain to be explored. This is true even for ferromagnets and antiferromagnets. In this work we considered a geometry where the magnetization was in the surface plane. It is also of interest to look at structures where the magnetization would be perpendicular to the surface plane, and indeed, if d_1 is very thin, this is the likely configuration. In addition other magnetic systems should be investigated. Many of the rare-earth metals are magnetic at low temperatures, with ferromagnetic, helical, or cone shaped ordering. It is expected that these materials could also be studied by appropriate structuring. We note that the present work is similar in spirit, though significantly different in details, to several earlier studies.[19,20] In particular, we mention the work by Sievers using a foil grating to obtain infrared signals from the magnetic excitations in Dy and Tb.[19]

*Permanent address: Dept. of Physics, University of Colorado at Colorado Springs, Colorado Springs, CO 80933-7150.

[1] T. Dumelow, T. J. Parker, S. R. P. Smith, and D. R. Tilley, Surf. Sci. Rep. **17**, 151 (1993).

[2] L. Remer, B. Lüthi, H. Sauer, R. Geick, and R. E. Camley, Phys. Rev. Lett. **56**, 2752 (1986).

[3] D. E. Brown, T. Dumelow, T. J. Parker, Kamsul Abraha, and D. R. Tilley, Phys. Rev. B **49**, 12 266 (1994).

[4] Kamsul Abraha, D. E. Brown, T. Dumelow, T. J. Parker, and D. R. Tilley, Phys. Rev. B **50**, 6808 (1994).

[5] V. M. Agranovich and V. E. Kravtsov, Solid State Commun. **55**, 373 (1985).

[6] N. Raj and D. R. Tilley, Solid State Commun. **55**, 533 (1985).

[7] N. Raj, R. E. Camley, and D. R. Tilley, J. Phys. C **20**, 5203 (1987).

[8] N. Raj and D. R. Tilley, Phys. Rev. B **36**, 7003 (1987).

[9] N. S. Almeida and D. L. Mills, Phys Rev. B **38**, 6698 (1988).

[10] R. E. Camley, M. G. Cottam, and D. R. Tilley, Solid State Commun. **81**, 571 (1992).

[11] Xuan-Zhang Wang and D. R. Tilley, Phys. Rev. B **50**, 13 472 (1994).

[12] N. S. Almeida and D. R. Tilley, Phys. Rev. B **43**, 11 145 (1991); Kamsul Abraha and D. R. Tilley, Infrared Phys. Technol. **35**, 681 (1994).

[13] R. L. Stamps and R. E. Camley, Phys. Rev. B **40**, 596 (1989).

[14] Z. Cellinski and B. Heinrich, J. Appl. Phys. **70**, 5935 (1991).

[15] L. R. Walker, in *Magnetism*, edited by G. T. Rado and H. Suhl (Academic, New York, 1963), p. 299.

[16] P. Krams, F. Lauks, R. L. Stamps, B. Hillebrands, and G. Güntherodt, Phys. Rev. Lett. **69**, 3674 (1992).

[17] F. C. Noertemann, R. L. Stamps, R. E. Camley, B. Hillebrands, and G. Güntherodt, Phys. Rev. B **47**, 3225 (1993).

[18] For a general review of superlattice excitations, see M. G. Cottam and D. R. Tilley, *Introduction to Surface and Superlattice Excitations* (Cambridge University Press, Cambridge, England, 1989).

[19] A. J. Sievers, J. Appl. Phys. **41**, 980 (1970).

[20] Yu. N. Kazantsev, M. V. Kostin, G. A. Kraftmakher, and V. V. Shevchenko, Sov. Tech. Phys. Lett. **17**, 792 (1991),